Caspase-8 is essential for maintaining chromosomal stability and suppressing B-cell lymphomagenesis

Anne Hakem,[1] Samah El Ghamrasni,[1,2] Georges Maire,[3] Benedicte Lemmers,[1] Jana Karaskova,[1] Andrea Jurisicova,[4] Otto Sanchez,[5] Jeremy Squire,[3] and Razqallah Hakem[1]

[1]Department of Medical Biophysics, University of Toronto and Ontario Cancer Institute, University Health Network, Toronto, ON; [2]Biology Department, University Med Ben Abdellah, Fez, Morocco; [3]Queen's University, Kingston, ON; [4]Samuel Lunenfeld Research Institute, Toronto, ON; and [5]University of Ontario Institute of Technology, Oshawa, ON

In addition to its proapoptotic function, caspase-8 is also important for several other processes, including suppressing necroptosis, cell migration, and immune cell survival. In the present study, we report that the loss of caspase-8 in B lymphocytes leads to B-cell malignancies and that the risk for these tumors is further enhanced in the absence of p53. We also report that deficiency of caspase-8 results in impaired cytokinesis and that *casp8*$^{-/-}$ lymphomas display remarkably elevated levels of chromosomal aberrations. Our data support an important role for caspase-8 in the maintenance of genomic integrity and highlight its tumor-suppressive function. (*Blood*. 2012;119(15):3495-3502)

Introduction

Deregulation of apoptosis has been linked to the pathogenesis of human cancer.[1] Caspases are essential for both the death receptor and the mitochondrial apoptotic pathways.[2] In addition to the critical role that caspase-8 (casp8) plays in the death receptor apoptotic pathway, mounting evidence also supports its nonapoptotic functions. casp8 is required for blood vessel formation during embryogenesis, survival of hematopoietic progenitors, and for mitogen- or antigen-induced T- and B-cell proliferation.[3-8] casp8 cleavage of the receptor interacting protein kinases (RIPKs) RIPK1 and RIPK3 results in their inhibition and in the suppression of necroptosis, a programmed necrotic cell death.[9-11] We and others have reported that mice lacking casp8 in the B-cell lineage (*CD19Cre;casp8*$^{fl/fl}$ mice; referred to herein as *bcasp8*$^{-/-}$ mice) display normal B-cell development and no abnormalities at a young age.[7,8] *casp8*$^{-/-}$ B cells are resistant to Fas killing and also display impaired activation in response to stimulation of TLR2, TLR3, and TLR4.[7,8]

Homozygous mutations of *CASP8* have been reported in 2 immunodeficient patients who also exhibited some features of the autoimmune lymphoproliferative syndrome.[4] Immunodeficiency was also observed in mice lacking casp8 in the T- or B-cell lineages.[5,7,8] Evidence also exists to support a possible role for CASP8 in human cancer. Loss of CASP8 expression because of hypermethylation of its promoter has been associated with human neuroblastomas with N-MYC amplification,[12] small-cell lung carcinoma,[13] and relapsed glioblastoma multiforme.[14] Inactivation of the *CASP8* gene by somatic mutations was also reported for human hepatocellular carcinomas and advanced gastric cancer.[15] In addition, loss of CASP8 has been associated with neuroblastoma metastasis.[16] Despite these data, compelling evidence is lacking to support a direct causal role for CASP8 inactivation in cancer development.

In the present study, we report that deficiency of casp8 in B cells and mouse embryonic fibroblasts (MEFs) results in impaired cytokinesis. Mice lacking casp8 in the B-cell lineage developed lymphomas with elevated chromosomal instability. Additional loss of p53 in the B cells of these mice further increased their cancer risk. Our data support casp8 as a tumor suppressor important for lymphomagenesis.

Methods

Mice

casp8$^{fl/fl}$ mice,[5] *p53*$^{fl/fl}$ mice[17] (obtained from the National Cancer Institute Mouse Repository), *Mx1-cre* mice,[18] and *CD19Cre* mice[19] were used to obtain *bcasp8*$^{-/-}$, *bcasp8*$^{-/-}$*p53*$^{-/-}$, *CD19Cre;p53*$^{fl/fl}$, and wild-type (*WT*) mice. All mice studied were in a mixed 129/J;C57BL/6;FVB genetic background and were genotyped by PCR (primer sequences and PCR conditions are available on request). All experiments were performed in compliance within the Ontario Cancer Institute animal care committee guidelines.

Flow cytometric analysis

Single-cell suspensions prepared from spleen and lymph nodes (LNs) were stained with the following Abs: anti-Thy.1, anti-B220, anti-CD43, anti-IgM, and anti-CD138. Stained cells were analyzed by flow cytometry (FACSCalibur; BD Biosciences) using CellQuest Version 5.3.2 software (Applied Biosystems). Cell death was examined using propidium iodide staining and FACS analysis. Dilution profiles of CFSE (Invitrogen) were examined by FACS to assess B-cell proliferation. Purified B cells were labeled with CFSE and cultured with lipopolysaccharides (LPS; 10 μg/mL; Sigma-Aldrich) for 48 hours in the presence or absence of necrostatin-1 (10μM; Calbiochem).

Submitted July 13, 2011; accepted January 24, 2012. Prepublished online as *Blood* First Edition paper, February 16, 2012; DOI 10.1182/blood-2011-07-367532.

The online version of this article contains a data supplement.

The publication costs of this article were defrayed in part by page charge payment. Therefore, and solely to indicate this fact, this article is hereby marked "advertisement" in accordance with 18 USC section 1734.

Western blot analysis

Western blot analysis was performed according to standard protocols. The following Abs were used: p53 (FL393; Santa Cruz Biotechnology), p21 (Santa Cruz Biotechnology), Puma (Cell Signaling Technology), and HRP-Actin (Santa Cruz Biotechnology).

Immunofluorescence

E1A-HRasV12–transformed and 3T3 MEFs were seeded onto coverslips in 24-well tissue-culture dishes; 18 hours later, cells were washed in PBS and fixed in 100% methanol for 10 minutes, and then blocked with 3% goat serum in PBS. Anti–γ-tubulin and anti–α-tubulin (Sigma-Aldrich) were used at a 1:1000 dilution and incubated with cells for 1 hour at room temperature. Labeling was revealed using anti–mouse Ab conjugated to FITC or PE (Molecular Probes). Cells were stained with 4′,6-diamidino-2-phenylindole (DAPI) for 5 minutes, and then mounted with Mowiol 4-88 (Calbiochem). The slides were observed under a Leica DMIRB fluorescence microscope equipped with digital camera (Leica DC 300RF). Images were acquired using Leica Image Manager Version 4.0.0 software. The confocal microscope (Zeiss) was also used with a 63× oil-immersion objective with a numerical aperture of 1.32. Untreated or 36-hour post-IgM activation B cells from *bcasp8*$^{-/-}$ and *WT* mice, either untreated or stimulated for 36 hours with anti-IgM, were seeded onto coverslips in 24-well tissue-culture dishes and fixed as described earlier.

ELISA

Serum levels of Ig and antinuclear Abs were determined using 5 pairs of 10- to 12-month-old *bcap8*$^{-/-}$ mice and *WT* littermates using mouse immunoglobulin isotype panel kits (Southern Biotechnology Associates) as described previously.[20] IL-6 serum levels were examined by ELISA (Fisher Scientific).

SKY analysis

Spectral karyotyping (SKY) was performed on metaphases according to the manufacturer's instructions (Applied Spectral Imaging) and as described previously.[21] A minimum of 10 metaphases were analyzed per sample. Metaphases not analyzed by SKY were stained with Giemsa according to the standard procedure. A minimal of 20 metaphases were analyzed per sample using HiSKY analysis software (Applied Spectral Imaging). Chromosomal abnormalities were scored as recommended by the International Standing Committee on Human Cytogenetic Nomenclature in 2009,[22] and following the recommendations by Savage et al.[23]

Histology

Paraffin sections of tumors and normal tissues were stained with H&E for histological analysis as described previously.[24] Images were captured with a 10× or 20× HCX lens on a Leica DM4000B microscope (Germany) equipped with a digital camera (Leica DC 300RF). Magnifications used were 10×/0.3, 20×/0.5, and 100×/1.30 at room temperature using Mowiol. Images were acquired using Leica Image Manager Version 4.0.0 Software. All digital images were imported into Photoshop CS4 (Adobe) and adjusted for gain, contrast, and γ settings.

Results

casp8 deficiency promotes B-cell lymphomagenesis

bcasp8$^{-/-}$ mice, which lack casp8 in the B-cell lineage, display no developmental defects and remain tumor free at young ages.[7,8] However, in the present study, we monitored cohorts of *bcasp8*$^{-/-}$ mice and their *WT* littermates for a period of 60 weeks and observed a shorter lifespan for *bcasp8*$^{-/-}$ mice (Figure 1A). Kaplan-Meier survival curves indicated that at the end of the observation period, 100% of *WT* mice (n = 12) were alive, compared with only 18 of 31 (58%) of *bcasp8*$^{-/-}$ mice ($P = .01$ by log-rank test). Sick *bcasp8*$^{-/-}$ mice displayed massive splenomegaly and lymphadenopathy, particularly of the mesenteric LNs

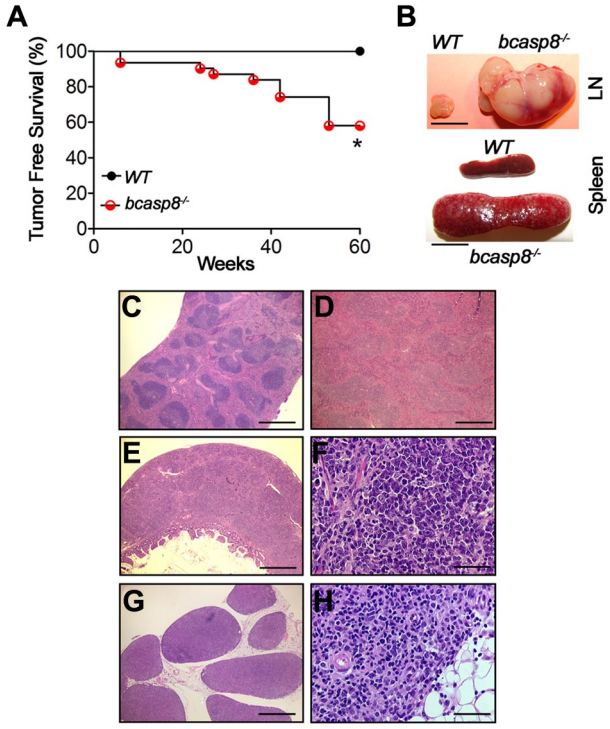

Figure 1. Deletion of casp8 in B cells leads to B-cell lymphomagenesis. (A) Kaplan-Meier analysis representing the percentage of tumor-free survival in cohorts of *WT* (n = 12) and *bcasp8*$^{-/-}$ (n = 31) mice. (B) Representative splenomegaly and lymphadenopathy displayed by *bcasp8*$^{-/-}$ sick mice. Bar indicates 1 cm. (C-D) H&E staining of the spleen of a *bcasp8*$^{-/-}$ sick mouse showing tumor cell infiltration predominantly affecting the red pulp. Bar indicates 500 μm. (E-F) H&E staining of intestine from a *bcasp8*$^{-/-}$ lymphoma bearing mouse. (E) Expansion of the Peyer patches, with thickening of the sub-mucosa and tumor invasion into the muscle layers and the mucosal lamina propria. Bar indicates 500 μm. (F) These tumors were composed of sheets of small lymphoid cells, many of which showed plasma cell phenotypes. Bar indicates 100 μm. (G-H) LNs infiltrated by tumors in which the normal architecture was partially or completely replaced by tumors and invading into the surrounding adipose tissue. Bar indicates 500 μm in panel G and 100 μm in panel H. *$P = .01$ for log-rank test between *WT* and *bcasp8*$^{-/-}$ curves.

(Figure 1B). Examination of H&E-stained sections of spleens and LNs of these mice indicated that 42% of mutant mice developed tumors by 1 year of age (Figure 1C-D and G-H).

The histology of these tumors showed similarities to human multiple myeloma, because the predominant observed cellular phenotype was mature plasma cells (Figure 1F), These tumors were found to be highly invasive and infiltrated multiple tissues and organs, including muscle adipose tissues, liver, bones, colon, and lungs (Figure 1E-H and supplemental Figure 1A-D, available on the *Blood* Web site; see the Supplemental Materials link at the top of the online article). However, we observed no osteolytic patterns that are characteristic of multiple myeloma (supplemental Figure 1E-F). Therefore, we characterized the tumors as "plasma-cell neoplasms."

Cytofluorometric analysis of these tumors indicated that they were negative for B220 and for CD138, a marker for plasma B cells (supplemental Figure 1G-H). We next examined the serum level of IL-6, a cytokine important for the differentiation and survival of plasma cells and involved in the development of plasma-cell neoplasms.[25,26] ELISA analysis indicated elevated IL-6 serum level in 10- to 12-month-old tumor-bearing *bcasp8*$^{-/-}$ mice (n = 5) compared with their *WT* (n = 5) littermates (167.1 vs 35.7 pg/mL, $P = .015$; supplemental Figure 2A). Because plasma-cell neoplasms can be classified based on their ability to secrete Ig,[26,27] we

also performed ELISA to examine the serum level of Ig in the tumor-bearing *bcasp8*$^{-/-}$ mice and their *WT* littermates. *Bim*$^{-/-}$ mice were used as positive controls because they develop a systemic lupus erythematosus–like syndrome and display hypergammaglobulinemia.[28] The level of serum Ig isotypes in *bcasp8*$^{-/-}$ mice was found to remain similar between *bcasp8*$^{-/-}$ mice and their *WT* littermates ($P > .05$; supplemental Figure 2B-E). In addition, consistent with the cancerous nature of their disease, *bcasp8*$^{-/-}$ mice displayed no increased serum level of antinuclear autoantibodies (*ANA*; supplemental Figure 2F). These data demonstrate that casp8 is a tumor suppressor important for suppressing B-cell lymphomagenesis.

casp8 deficiency preferentially predisposes for B-cell lymphomagenesis

To examine tumor specificity associated with casp8 deficiency, we used the *Mx1-cre* transgene to delete casp8 in various tissues. *Mx1-Cre* mice express the transgene Cre under the control of the IFN-α/β–inducible *Mx1* promoter.[18] Whereas injection of the synthetic double-stranded RNA pI-pC is used to induce IFN expression to trigger Cre expression, several studies have indicated leakiness of the *Mx1-Cre* transgene and showed that its expression is spontaneously induced by endogenous IFN in the absence of any pI-pC injection.[29-31] We therefore killed a cohort of 16- to 18-month-old *Mx1-cre*;*casp8*$^{fl/fl}$ mice (n = 8) and *Mx1-cre* littermates (n = 5) that had not been injected previously with pI-pC. PCR analysis of genomic DNA indicated variable levels of casp8 deletion in tested tissues, including spleen, LNs, and liver (supplemental Figure 3A). Partial loss of the casp8 protein was confirmed by immunostaining of spleen sections from *Mx1-cre*;*casp8*$^{fl/fl}$ mice with anti-casp8 polyclonal Ab (supplemental Figure 3B-D). Whereas no tumors were observed in the *Mx1-cre* littermates, 7 of 8 (87.5%) *Mx1-cre*;*casp8*$^{fl/fl}$ mice examined showed the presence of highly invasive lymphomas of B-cell origin, similar to *bcasp8*$^{-/-}$ mice (supplemental Figure 4). Therefore, whereas casp8 was deleted in several tissues in *Mx1-cre;casp8*$^{fl/fl}$ mice, only B-cell lymphomas were observed in these mice, suggesting that casp8 deficiency preferentially predisposes for B-cell malignancy.

Cooperation of casp8 and p53 in tumor suppression

p53 is critical for several cellular processes, including apoptosis, and is the most frequently inactivated tumor suppressor in human cancer.[32,33] To examine whether functional interactions exist between p53 and casp8, we crossed *bcasp8*$^{-/-}$ mice to *p53*$^{fl/fl}$ mice[17] and generated *CD19Cre;casp8*$^{fl/fl}$;*p53*$^{fl/fl}$ (*bcasp8*$^{-/-}$*p53*$^{-/-}$) mice. Double mutant mice were viable and at 6-10 weeks of age, were healthy and displayed no difference in the number or distribution of their B cells or other immune cells compared with single mutant and *WT* littermates (supplemental Figure 5A-B).

The effects of p53 inactivation on tumorigenesis of *bcasp8*$^{-/-}$ mice was examined by monitoring cohorts of *CD19Cre;p53*$^{fl/fl}$ mice (n = 10) and *bcasp8*$^{-/-}$*p53*$^{-/-}$ mice (n = 30) for a period of 60 weeks. Two of 10 monitored *CD19Cre;p53*$^{fl/fl}$ mice developed B-cell lymphomas with late latency and died at the age of 54 and 57 weeks, respectively (Figure 2A). In contrast, *bcasp8*$^{-/-}$*p53*$^{-/-}$ mice had a significantly shorter life span and higher frequency of tumors compared with *bcasp8*$^{-/-}$ mice ($P = .04$ by log-rank test) and *CD19Cre;p53*$^{fl/fl}$ mice ($P = .015$ by log-rank test).

Examination of H&E–stained sections of spleen, LNs, lungs, liver, and kidneys from moribund *bcasp8*$^{-/-}$*p53*$^{-/-}$ mice indicated

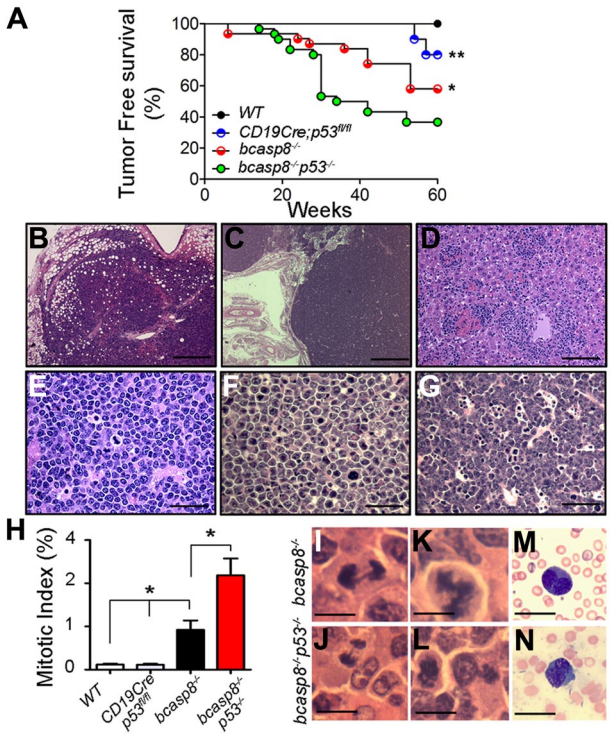

Figure 2. Increased frequency and shorter latency of B-cell lymphomagenesis in the absence of casp8 and p53. Kaplan-Meier analysis of the tumor-free survival in cohorts of *WT* (n = 12), *bcasp8*$^{-/-}$ (n = 31), *CD19Cre;p53*$^{fl/fl}$ (n = 10), and *bcasp8*$^{-/-}$*p53*$^{-/-}$ (n = 30) mice. *$P = .04$ for the log-rank test between survival curves of *bcasp8*$^{-/-}$*p53*$^{-/-}$ and *bcasp8*$^{-/-}$ mice and **$P = .015$ for *bcasp8*$^{-/-}$*p53*$^{-/-}$ and *CD19Cre;p53*$^{fl/fl}$ mice. (B-C) H&E staining of LNs infiltrated with proliferating *bcasp8*$^{-/-}$*p53*$^{-/-}$ tumor cells. Bar indicates 250 μm in panel B and 500 μm in panel C. (D) *bcasp8*$^{-/-}$*p53*$^{-/-}$ lymphomas infiltrating hepatic sinusoids and periportal spaces. Bar indicates 100 μm. (E-G) High magnification showing tumors with high mitotic index. Bar indicates 50 μm. (H) Mitotic index of tumors from *WT* (n = 5), *p53*$^{-/-}$ (n = 3), *bcasp8*$^{-/-}$ (n = 3), and *bcasp8*$^{-/-}$*p53*$^{-/-}$(n = 3) mice. Ten different fields were counted for each tumor. *Student *t* test indicated statistical significance. (I-J) Representative anaphase bridges in H&E-stained tumors from *bcasp8*$^{-/-}$ mice (I) and *bcasp8*$^{-/-}$*p53*$^{-/-}$ mice (J). (K) Representative abnormal multipolar metaphase observed in H&E-stained tumors from *bcasp8*$^{-/-}$ mice. (L) Representative abnormal asymmetric metaphase observed in H&E-stained tumors from *bcasp8*$^{-/-}$*p53*$^{-/-}$mice. (M-N) Binucleated tumor cells in blood smear (N) and touch smear from kidney of *bcasp8*$^{-/-}$ mice. Bar indicates 10 μm in panels I through N.

that these mutants developed plasma-cell neoplasms that were morphologically similar to those observed in *bcasp8*$^{-/-}$ mice. In addition, similar to *bcasp8*$^{-/-}$ tumors, *bcasp8*$^{-/-}$*p53*$^{-/-}$ tumors were also negative for CD138. However, in contrast to *bcasp8*$^{-/-}$ tumors, which were negative for B220, *bcasp8*$^{-/-}$*p53*$^{-/-}$ lymphomas expressed a low level of B220 (supplemental Figure 5C-D). The LNs of tumor-bearing *bcasp8*$^{-/-}$*p53*$^{-/-}$ mice were enlarged by the presence of proliferating tumor cells, with clear invasion of surrounding adipose tissues (Figure 2B) and alteration of the normal nodal architecture (Figure 2C). Tumor infiltration was also evident in hepatic sinusoids and periportal spaces (Figure 2D). At high magnification, tumors were composed of plasma cells at various stages of differentiation (Figure 2E) and displayed elevated numbers of mitotic figures (Figure 2E-G). Examination of the mitotic index of *bcasp8*$^{-/-}$*p53*$^{-/-}$ tumors indicated that it was significantly higher compared with *bcasp8*$^{-/-}$ tumors ($P = .007$), and that both tumors were highly proliferating compared with *WT* and *p53*$^{-/-}$ B cells (Figure 2H). We conclude that the loss of p53 facilitates B-cell lymphomagenesis associated with casp8 deficiency.

Impaired cytokinesis in the absence of casp8

Failure of cytokinesis is frequently associated with human cancer and has been reported to result from various defects, including anaphase bridges and multipolar and abnormal mitosis.[34-37] Interestingly, H&E–stained tumor sections from *bcasp8*$^{-/-}$ mice and *bcasp8*$^{-/-}$*p53*$^{-/-}$ mice displayed mitotic cells with anaphase bridges (Figure 2I-J) and multipolar or abnormal mitosis (Figure 2K-L and supplemental Figure 6A). Multinucleated cells, a common result of cytokinesis failure, were also observed in blood smears of tumor-bearing *bcasp8*$^{-/-}$ mice (Figure 2M) and in touch smears of kidneys infiltrated with *bcasp8*$^{-/-}$ tumors (Figure 2N). Therefore, we conclude that tumors deficient for casp8 display cytokinesis defects.

To determine whether cytokinesis defects observed in *casp8* mutants preceded tumor development, we have examined H&E–stained spleen sections of tumor-free *WT* and *bcasp8*$^{-/-}$ mice for features of cytokinesis failure. Whereas no abnormalities of cytokinesis were observed in the spleens of *WT* mice, anaphase bridges and multipolar metaphases were readily observed in the spleens of tumor-free *bcasp8*$^{-/-}$ mice (supplemental Figure 6B-F). These data suggest that cytokinesis defects associated with the absence of casp8 precede B-cell lymphomagenesis in mutant mice.

To further investigate the mechanisms that lead to B-cell malignancy in the absence of casp8, we examined levels of B-cell proliferation and death in healthy *bcasp8*$^{-/-}$ mice and their *WT* littermates. Whereas we observed no defect in the proliferation of B cells from *bcasp8*$^{-/-}$ mice (supplemental Figure 7A), higher level of death was observed in *bcasp8*$^{-/-}$ B cells compared with *WT* controls both under untreated conditions and after IgM activation (supplemental Figure 7B-D).

Centrosomes are critical for microtubule organization and function and for chromosome segregation and cytokinesis.[34] We therefore examined centrosome numbers in *WT* and *casp8*$^{-/-}$ B cells. Because the loss of casp8 has been shown previously to increase the transformation rate of SV40 T-antigen–immortalized *casp8*$^{-/-}$ MEFs at their late passages,[38] we also examined centrosome numbers in *E1A-HRasV12*–transformed and 3T3-immortalized *WT* and *casp8*$^{-/-}$ MEFs. In contrast to *WT* controls, which predominantly displayed a single centrosome, an increased frequency of multiple centrosomes was observed in *casp8*$^{-/-}$ B cells and MEFs (Figure 3A-C and supplemental Figure 8A-E and I). Whereas we observed no *WT* B cells with more than 2 centrosomes, nearly 20% of the examined *casp8*$^{-/-}$ B cells displayed 3 or more centrosomes (Figure 3B). The number of MEFs with 3 or more centrosomes was also highly increased in the absence of casp8 (supplemental Figure 8I).

Excess of functional centrosomes can lead to aberrant formation of multipolar spindles.[34] Consistent with the supernumerary centrosomes of *casp8*$^{-/-}$ B cells and MEFs, these cells displayed multipolar mitotic spindles (Figure 3C and supplemental Figure 8C-E) and binucleate cells (Figure 3D-E and supplemental Figure 8F). In addition, micronuclei, which can result from abnormal mitosis and cytokinesis,[39] were present at a significantly higher frequency in *casp8*$^{-/-}$ B cells and MEFs compared with *WT* controls (Figure 3F-G and supplemental Figure 8G,J).

The final step of cytokinesis, "abscission," consists of cleavage of the cytoplasmic bridge containing the midbody that connects the 2 daughter cells.[34,36] Because elongated intercellular bridges are characteristic of defective cytokinesis, we examined their presence in *casp8*$^{-/-}$ B cells, *casp8*$^{-/-}$ MEFs, and *WT* controls after immunofluorescence staining with Abs for α-tubulin. The frequency of intercellular bridges was significantly increased in both

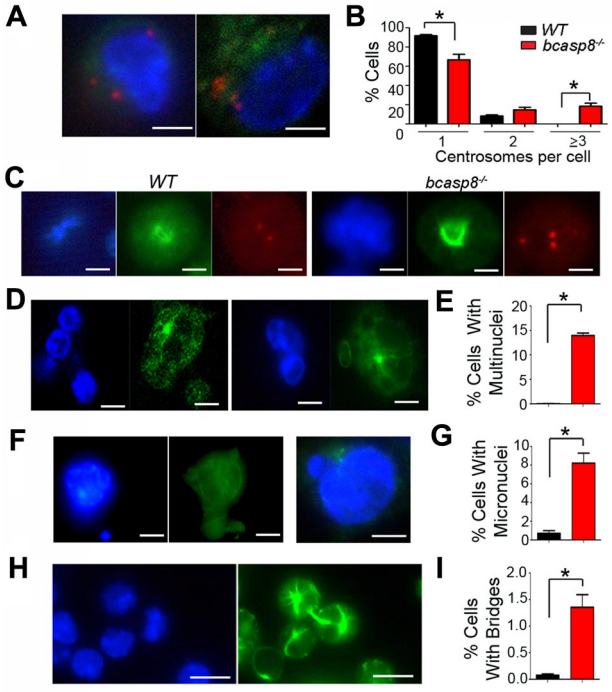

Figure 3. Cytokinesis defects in *casp8*$^{-/-}$ B cells. (A) Two independent *bcasp8*$^{-/-}$ B-cell lymphomas were immunostained with anti–γ-tubulin and counterstained with DAPI to visualize centrosomes and DNA, respectively. Bar indicates 10 μm. (B) Graphs depicting the percentages of *WT* and *bcasp8*$^{-/-}$ tumors with 1, 2, or ≥ 3 centrosomes. (C) Abnormal spindle pole formation and chromosomal segregation defects in *casp8*$^{-/-}$ B cells. B cells from *WT* mice are also shown. Cells were immunostained with anti–γ-tubulin (red) to visualize centrosomes, anti–α-tubulin (green) to visualize mitotic spindles, and counterstained with DAPI (blue) to visualize chromatin. Bar indicates 10 μm. (D) Two independent *bcasp8*$^{-/-}$ B-cell lymphomas were immunostained with anti–α-tubulin and counterstained with DAPI to visualize multinucleated cells. Bar indicates 10 μm. (E) Graphs depicting the percentages of *WT* and *bcasp8*$^{-/-}$ B-cell lymphomas with multinuclei. (F) Two independent *bcasp8*$^{-/-}$ B-cell lymphomas were immunostained with anti–α-tubulin and counterstained with DAPI to visualize micronuclei. Bar indicates 10 μm. (G) Graphs depicting the percentages of *WT* and *bcasp8*$^{-/-}$ B-cell lymphomas with micronuclei. (H) *bcasp8*$^{-/-}$ B-cell lymphomas were immunostained with anti–α-tubulin and counterstained with DAPI to visualize cytoplasmic bridges. Bar indicates 25 μm. (I) Graphs depicting the percentages of *WT* and *bcasp8*$^{-/-}$ B-cell lymphomas displaying cytoplasmic bridges. Data are presented as the means ± SD of 4 independent experiments. *$P < .05$ by Student *t* test.

casp8$^{-/-}$ B cells and *casp8*$^{-/-}$ MEFs compared with *WT* controls (Figure 3H-I and supplemental Figure 8H-K). These data indicate increased frequency of cytokinesis failure in the absence of casp8.

Aneuploidy and elevated structural chromosomal aberrations in tumors deficient in casp8

Aneuploidy and structural chromosomal aberrations are hallmarks of human cancers.[34,40] Aneuploidy is frequently associated with impaired mitotic checkpoint signaling, sister chromatid cohesion, and multipolar mitotic spindles, and can also result from chromosomal instability.[34] Conversely, chromosomal instability has been shown to result from defects in several cellular processes, including the presence of extra centrosomes.[34,35,41] Because supernumerary centrosomes and cytokinesis defects were observed in *casp8*$^{-/-}$ cells, we used SKY analysis to examine the level of chromosomal instability in *bcasp8*$^{-/-}$ and *bcasp8*$^{-/-}$*p53*$^{-/-}$ primary tumors. Complex karyotypes with elevated frequencies of numerical and structural chromosomal abnormalities were observed in *bcasp8*$^{-/-}$ tumors (Figure 4A-B and Table 1). All metaphases from *bcasp8*$^{-/-}$ tumors were aneuploid and had an overall near-tetraploid pattern. The modal chromosomal number of these tumors varied from

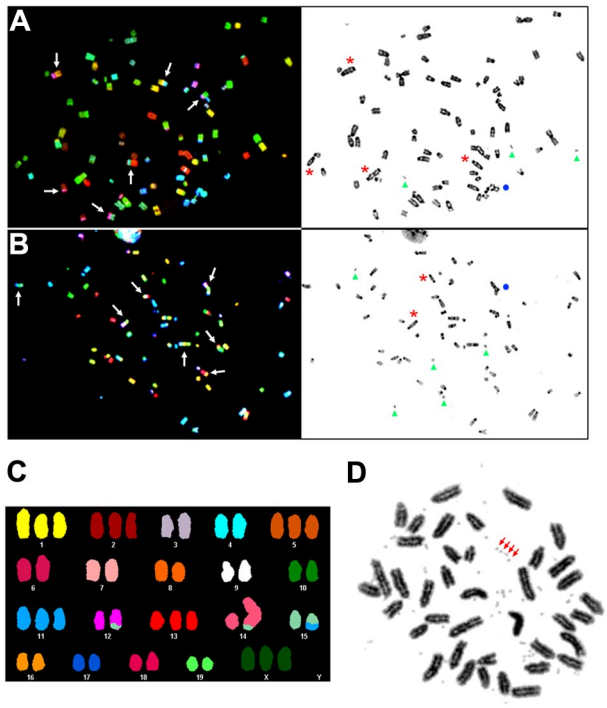

Figure 4. Elevated genomic instability in casp8-deficient B-cell lymphomas. (A-B) The genomic instability of *bcasp8*$^{-/-}$ B-cell lymphomas (A, tumor 1; and B, tumor 2) was examined by SKY. The left panels show metaphases hybridized with the SKY probe. The matching inverted DAPI staining is shown in the right panels. A multitude of numerical and complex structural rearrangements were observed: dicentric chromosome (*); acentric chromosome (arrowhead), triradial (●), and translocation (arrow). (C) Representative SKY karyotype of *bcasp8*$^{-/-}$*p53*$^{-/-}$ tumors showing aneuploidy and chromosomal translocations (46,XX,+X,+1,+2,+5,+11,der(12)t(12;15)(D;F),+13,der(14)dup(14)(?)t(14;15)(E;F),der(15)t(11;15)(E1;D1). (D) Representative diploid metaphase of a lymphoma from *bcasp8*$^{-/-}$*p53*$^{-/-}$ mice. The presence of numerous double-minute chromosomes is evident (representatives are indicated with arrows).

67 (hypertriploid) to 84 (hypertetraploid). Furthermore, a high proportion of the chromosomes of *bcasp8*$^{-/-}$ tumors displayed structural abnormalities. One fourth of these chromosomes showed centromeric abnormalities (eg, acentric, multicentric, and double-minute chromosomes). Intrachromosomal rearrangements were also observed in *bcasp8*$^{-/-}$ tumors, because 12% of their chromosomes displayed either duplication or deletion, and 1-3 ring chromosomes were detected in 4 of the 10 metaphases analyzed. Abnormal chromosomes derived from complex translocation patterns involving 2-3 different chromosomal origins were also frequently observed in *bcasp8*$^{-/-}$ tumors, with an average number of 70 abnormally fused chromosomal segments per metaphase. Triradial chromosomes (1-2) were also observed in 50% of the *bcasp8*$^{-/-}$ tumor metaphases examined. Only a minority of chromosomes in *bcasp8*$^{-/-}$ tumors appeared normal by SKY and inverted DAPI analysis.

Elevated level of chromosomal instability was also observed in *bcasp8*$^{-/-}$*p53*$^{-/-}$ tumors, with their chromosome content near-diploid to near-triploid (Figure 4C and supplemental Table 1). Structural rearrangements were limited to the presence of 2-3 abnormally fused chromosomal segments per metaphase, and most of them were clonal. Double-minute chromosomes were also observed (Figure 4D). In contrast to *bcasp8*$^{-/-}$ tumors, no dicentric, multicentric, triradial, or ring chromosomes were detected in *bcasp8*$^{-/-}$*p53*$^{-/-}$ tumors. These data indicate increased chromosomal instability in lymphomas deficient for casp8.

Responses of casp8-deficient lymphomas to radiation and LPS treatment

Because it is important for cancer therapy, we examined the response of casp8-deficient tumors to irradiation (IR). *bcasp8*$^{-/-}$ and *bcasp8*$^{-/-}$*p53*$^{-/-}$ B-cell lymphomas were irradiated (6 Gy) and their survival level examined 24 hours after IR. As expected based on the important role that p53 plays in the DNA-damage response, B-cell lymphomas from *bcasp8*$^{-/-}$*p53*$^{-/-}$ mice were highly radioresistant (Figure 5A). However, whereas some *bcasp8*$^{-/-}$ B-cell lymphomas were highly radiosensitive, others

Table 1. Chromosomal instability of *bcasp8*$^{-/-}$ lymphomas

	Cell 1	Cell 2	Cell 3	Cell 4	Cell 5	Range	Average
***bcasp8*$^{-/-}$ tumor no. 1**							
No. of chromosomes	84	75	82	83	83	75-84	81.4
Dicentrics/tetracentrics	14	9	19	17	15	9-19	14.8
Acentrics/double minute	8	12	12	17	9	8-17	11.6
Chromosome with deletion	16	5	10	14	15	5-16	12
Chromosome with probable duplication	2	1	0	1	1	0-2	1
Tri-radials	1	1	0	0	1	0-1	0.6
Ring chromosomes	0	0	0	3	1	0-3	0.8
Abnormally fused chromosome segments	42	25	45	40	32	25-45	36.8
Total no. of changes per cell	83	53	86	92	74	53-92	77.6
Total no. of changes per chromosome	0.99	0.71	1.05	1.11	0.89		0.95
***bcasp8*$^{-/-}$ tumor no. 2**							
No. of chromosomes	81	79	80	87	67	67-81	78.8
Dicentrics/tetracentrics	11	18	15	14	10	10-18	13.6
Acentrics/double minute	7	11	17	16	10	7-16	12.2
Chromosome with deletion	14	8	7	10	8	7-14	9.4
Chromosome with probable duplication	0	0	0	0	0	0	0
Tri-radials	0	0	1	0	2	0-2	0.6
Ring chromosomes	0	0	0	1	1	0-1	0.5
Abnormally fused chromosome segments	26	26	20	36	18	20-36	25.2
Total no. of changes per cell	58	63	60	77	49	49-77	61.4
Total no. of changes per chromosome	0.72	0.8	0.75	0.89	0.73		0.78

Chromosomal abnormalities are described as recommended by International Standing Committee on Human Cytogenetic Nomenclature[22] and following the recommendations of Savage et al.[23] The abnormally fused chromosomal segments are identified as per a SKY color variation on a derivative chromosome (eg, a derivative chromosome composed of 3 different chromosome segments would have a score of 2).

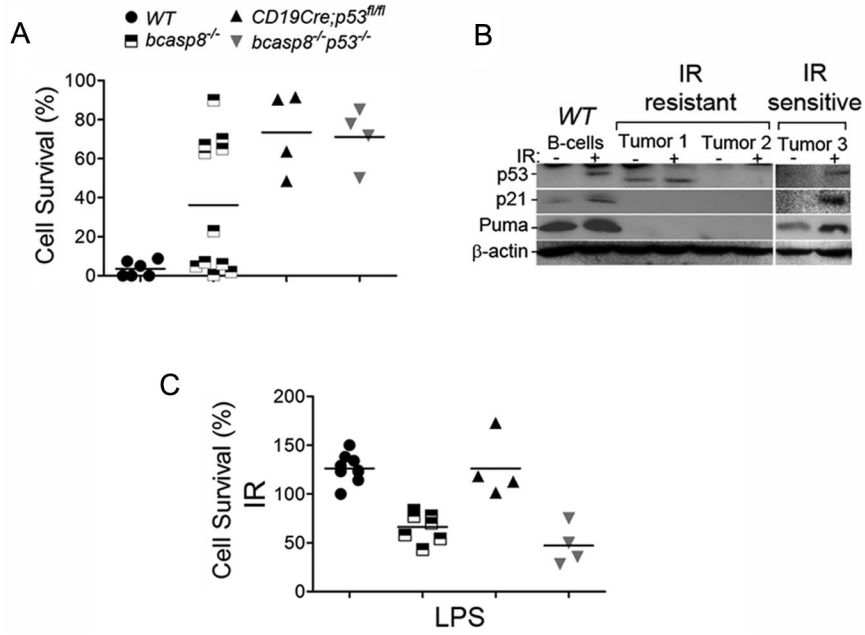

Figure 5. Sensitivity of *casp8*$^{-/-}$ lymphomas to radiation and LPS-induced killing. (A) B-cell lymphomas from *bcasp8*$^{-/-}$ mice (n = 12) and *bcasp8*$^{-/-}$*p53*$^{-/-}$ mice (n = 4) and B cells from *WT* mice (n = 5) and *p53*$^{-/-}$ mice (n = 4) were irradiated and their survival level examined 24 hours later using propidium iodide staining. (B) Expression of p53, p21, and Puma in *bcasp8*$^{-/-}$ lymphomas and normal *WT* B cells was examined using Western blotting. Cells were either untreated or irradiated (6 Gy) and examined 4 hours after IR. (C) B-cell lymphomas from *bcasp8*$^{-/-}$ mice (n = 8) and *bcasp8*$^{-/-}$*p53*$^{-/-}$ mice (n = 4) and B cells from *WT* mice (n = 9) and *CD19Cre;p53*$^{fl/fl}$ mice (n = 4) were treated with LPS and their survival level examined 24 hours later. $^{*}P < .05$ for *bcasp8*$^{-/-}$ and *bcasp8*$^{-/-}$*p53*$^{-/-}$ samples versus *WT* and *CD19Cre;p53*$^{fl/fl}$ samples by Student *t* test.

displayed elevated radioresistance (Figure 5A). p53 is frequently inactivated in tumors through various mechanisms, and this inactivation leads to radioresistance. Therefore, we examined whether differences in p53 responses could contribute to the differential IR sensitivity observed with *bcasp8*$^{-/-}$ B-cell lymphomas. These tumors and *WT* splenocytes were left untreated or were irradiated (6 Gy) and their level of p53 examined 4 hours later. DNA damage induces activation of p53 that transactivates several target genes.[42] Therefore, we also examined the expression level of p21 and Puma, 2 downstream targets of p53 involved in cell-cycle control and apoptosis, respectively. Western blot analysis showed that whereas radiosensitive *bcasp8*$^{-/-}$ B-cell lymphomas displayed IR-induced expression of p53, p21, and Puma, radioresistant lymphomas failed to increase the expression of p53 or its targets, p21 and Puma, suggesting that loss of p53 activation in these tumors is the cause of their radioresistance (Figure 5B).

casp8$^{-/-}$ B cells display impaired TLR signaling.[7,8] Whereas LPS stimulation of TLR4 induced proliferation of *WT* B cells, it also promoted the killing of *casp8*$^{-/-}$ B cells. In addition to promoting apoptosis, casp8 has also been shown to inhibit necroptosis.[9-11] This type of cell death takes place in the absence of casp8, and recent studies have demonstrated that genetic deletion of the necroptotic kinase RIPK3 fully rescues embryonic lethality of *casp8*$^{-/-}$ mice and restores their impaired T-cell homeostasis.[43,44] However, whereas necrostatin-1 (Nec1), a specific inhibitor of RIPK1 and necroptosis, was able to fully rescue the survival and proliferation of *casp8*$^{-/-}$ T cells,[45] it failed to rescue survival or proliferation of LPS-stimulated *casp8*$^{-/-}$ B cells (supplemental Figure 9). Therefore, TLR4 stimulation results in the killing of *casp8*$^{-/-}$ B cells in a necroptosis-independent manner.

We next examined whether LPS-induced killing of B cells in the absence of casp8 can be exploited to kill *bcasp8*$^{-/-}$ and *bcasp8*$^{-/-}$*p53*$^{-/-}$ B-cell lymphomas. These tumors, as well as B cells from healthy *WT* mice and *p53*$^{-/-}$ littermates, were stimulated ex vivo with LPS for 24 hours and their survival levels determined using the annexin V/propidium iodide assay. Similar to *casp8*$^{-/-}$ B cells,[7] the survival of *bcasp8*$^{-/-}$ and *bcasp8*$^{-/-}$*p53*$^{-/-}$ B-cell lymphomas was significantly reduced in the presence of LPS (Figure 5C). Therefore, we conclude that whereas a subset of *casp8*$^{-/-}$ lymphomas is radiosensitive, other tumors display impaired p53 activation and are radioresistant. In contrast, all casp8-deficient B-cell lymphomas display increased death sensitivity to LPS in a p53-independent manner.

Discussion

Whereas decreased expression of CASP8 or its somatic mutations have been reported in human cancer,[12-15] and loss of casp8 has been shown to facilitate cellular transformation in vitro,[38] there is currently no clear evidence to support the idea that in vivo deregulation of CASP8 may promote the initiation of cancer. Using 3 different mouse models, we demonstrate in the present study that the loss of casp8 in B cells is sufficient to lead to B-cell lymphomagenesis. Our data also indicate that p53 deficiency further exacerbates B-cell lymphomagenesis associated with casp8 deficiency. Consistent with the proposed function for CASP8 as a suppressor of metastasis,[16] lymphomas developed in *bcasp8*$^{-/-}$, *Mx1-cre;casp8*$^{fl/fl}$, and *bcasp8*$^{-/-}$*p53*$^{-/-}$ mice were highly invasive.

In contrast to mice lacking casp8 in the B-cell lineage, no spontaneous tumorigenesis was observed in mice with the *casp8* mutation specifically targeted to the T-cell lineage[24] or mammary epithelial cells (A.H., unpublished data, December 2009). In addition, whereas *Mx1-cre;casp8*$^{fl/fl}$ displayed deletion of casp8 in various tissues and cell types, these mice only developed B-cell lymphomas. Whereas the mechanisms for this tumor type specificity associated with casp8 deficiency remain unclear, increased necroptosis reported for casp8 deficiency in certain cell types might contribute to these differences in cancer predisposition. For example, impaired proliferation of *casp8*$^{-/-}$ T cells is rescued by the necroptosis inhibitor Nec1,[45] and defective T-cell homeostasis associated with *casp8* mutation is rescued in the Ripk3-null background.[43,44] In contrast, our data indicate that loss of casp8 in B cells does not lead to their death by necroptosis. Therefore, it remains possible that necroptosis associated with casp8 deficiency in certain cell types and tissues might suppress their tumorigenic risks.

In the present study, we report that the loss of casp8 in B cells and MEFs is accompanied by increased frequency of cytokinesis defects. We also report elevated chromosomal instability in *casp8*$^{-/-}$ lymphomas. Because cytokinesis failure and chromosomal instability play important roles in cancer development,[34,35,46] we propose that they contribute to the B-cell lymphomagenesis associated with casp8 deficiency. However, because of the existence of a close reciprocal relationship between cytokinesis failure and chromosomal instability,[34] the specific contribution of each of these defects to the malignancy of *bcasp8*$^{-/-}$ mice requires further investigation. Nevertheless, whereas we observed no chromosomal instability in B cells from young, tumor-free *bcasp8*$^{-/-}$ mice, these B cells displayed increased frequency of cytokinesis defects. Therefore, the impaired cytokinesis associated with casp8 deficiency in B cells might precede chromosomal instability and the malignant transformation of these cells.

The numerical and structural chromosomal abnormalities observed in *bcasp8*$^{-/-}$*p53*$^{-/-}$ lymphomas were clonal and less complex compared with those observed with *bcasp8*$^{-/-}$ lymphomas. The mechanisms for these differences are currently unknown; however, we speculate that the different status of p53 and the different stages of these lymphomas are likely to contribute to their different pattern of chromosomal abnormalities.

Our data indicate that a deficiency of p53 promotes the development of *casp8*$^{-/-}$ B-cell lymphomas, and that approximately half of examined *bcas8*$^{-/-}$ tumors are radioresistant and display impaired activation of p53. Therefore, it is possible that the DNA-damage response, including p53 activation, promotes the elimination of aberrant *casp8*$^{-/-}$ B cells carrying genomic instability and leads to the suppression of cancer risks associated with this mutation.

In conclusion, our data demonstrate that casp8 functions as a tumor suppressor. This novel function of casp8, together with the previously reported immunodeficiency and developmental defects associated with its deficiency, all highlight the importance of this caspase in diseases such as cancer.

Acknowledgments

The authors thank M. Woo, V. Stambolic, L. Pelletier, L. Salmena, and J. Li for helpful discussions and Dr Klaus Rajewsky for providing us with the *Mx1-cre* mouse line.

This work was supported by the Leukemia & Lymphoma Society of Canada (to R.H.), the Canadian Institute of Health Research (to R.H.), and the Canadian Cancer Society (to J.S.).

Authorship

Contribution: A.H., S.E.G., G.M., B.L., J.K., and A.J. conducted the experiments and performed the data analyses; O.S., J.S., and R.H. performed the data analyses; and A.H. and R.H. designed the experiments and wrote the manuscript.

Conflict-of-interest disclosure: The authors declare no competing financial interests.

Correspondence: Razq Hakem, PhD, Professor, Department of Medical Biophysics and Department of Immunology, University of Toronto University Health Network, Ontario Cancer Institute, 610 University Avenue, Room 10-622, Toronto, ON, M5G 2M9 Canada; e-mail: rhakem@uhnres.utoronto.ca; or Anne Hakem, PhD, University Health Network, Ontario Cancer Institute, 610 University Ave, Room 10-622, Toronto, ON, M5G 2M9 Canada; e-mail: ahakem@uhnres.utoronto.ca.

References

1. Cotter TG. Apoptosis and cancer: the genesis of a research field. *Nat Rev Cancer.* 2009;9(7):501-507.
2. Krammer PH, Arnold R, Lavrik IN. Life and death in peripheral T cells. *Nat Rev Immunol.* 2007;7(7):532-542.
3. Su H, Bidere N, Zheng L, et al. Requirement for caspase-8 in NF-kappaB activation by antigen receptor. *Science.* 2005;307(5714):1465-1468.
4. Chun HJ, Zheng L, Ahmad M, et al. Pleiotropic defects in lymphocyte activation caused by caspase-8 mutations lead to human immunodeficiency. *Nature.* 2002;419(6905):395-399.
5. Salmena L, Lemmers B, Hakem A, et al. Essential role for caspase 8 in T-cell homeostasis and T-cell-mediated immunity. *Genes Dev.* 2003;17(7):883-895.
6. Kang TB, Ben-Moshe T, Varfolomeev EE, et al. Caspase-8 serves both apoptotic and nonapoptotic roles. *J Immunol.* 2004;173(5):2976-2984.
7. Lemmers B, Salmena L, Bidere N, et al. Essential role for caspase-8 in Toll-like receptors and NFkappaB signaling. *J Biol Chem.* 2007;282(10):7416-7423.
8. Beisner DR, Ch'en IL, Kolla RV, Hoffmann A, Hedrick SM. Cutting edge: innate immunity conferred by B cells is regulated by caspase-8. *J Immunol.* 2005;175(6):3469-3473.
9. Wilson NS, Dixit V, Ashkenazi A. Death receptor signal transducers: nodes of coordination in immune signaling networks. *Nat Immunol.* 2009;10(4):348-355.
10. Vandenabeele P, Galluzzi L, Vanden Berghe T, Kroemer G. Molecular mechanisms of necroptosis: an ordered cellular explosion. *Nat Rev Mol Cell Biol.* 2010;11(10):700-714.
11. Zhang DW, Shao J, Lin J, et al. RIP3, an energy metabolism regulator that switches TNF-induced cell death from apoptosis to necrosis. *Science.* 2009;325(5938):332-336.
12. Teitz T, Wei T, Valentine MB, et al. Caspase 8 is deleted or silenced preferentially in childhood neuroblastomas with amplification of MYCN. *Nat Med.* 2000;6(5):529-535.
13. Hopkins-Donaldson S, Ziegler A, Kurtz S, et al. Silencing of death receptor and caspase-8 expression in small cell lung carcinoma cell lines and tumors by DNA methylation. *Cell Death Differ.* 2003;10(3):356-364.
14. Martinez R, Setien F, Voelter C, et al. CpG island promoter hypermethylation of the pro-apoptotic gene caspase-8 is a common hallmark of relapsed glioblastoma multiforme. *Carcinogenesis.* 2007;28(6):1264-1268.
15. Soung YH, Lee JW, Kim SY, et al. Caspase-8 gene is frequently inactivated by the frameshift somatic mutation 1225_1226delTG in hepatocellular carcinomas. *Oncogene.* 2005;24(1):141-147.
16. Stupack DG, Teitz T, Potter MD, et al. Potentiation of neuroblastoma metastasis by loss of caspase-8. *Nature.* 2006;439(7072):95-99.
17. Jonkers J, Meuwissen R, van der Gulden H, Peterse H, van der Valk M, Berns A. Synergistic tumor suppressor activity of BRCA2 and p53 in a conditional mouse model for breast cancer. *Nat Genet.* 2001;29(4):418-425.
18. Kühn R, Schwenk F, Aguet M, Rajewsky K. Inducible gene targeting in mice. *Science.* 1995;269(5229):1427-1429.
19. Rickert RC, Roes J, Rajewsky K. B lymphocyte-specific, Cre-mediated mutagenesis in mice. *Nucleic Acids Res.* 1997;25(6):1317-1318.
20. Li L, Halaby MJ, Hakem A, et al. Rnf8 deficiency impairs class switch recombination, spermatogenesis, and genomic integrity and predisposes for cancer. *J Exp Med.* 2010;207(5):983-997.
21. Bayani J, Zielenska M, Marrano P, et al. Molecular cytogenetic analysis of medulloblastomas and supratentorial primitive neuroectodermal tumors by using conventional banding, comparative genomic hybridization, and spectral karyotyping. *J Neurosurg.* 2000;93(3):437-448.
22. Shaffer GL, Slovak LM, Campbell JL. *An International System for Human Cytogenetic Nomenclature.* Basel, Switzerland: Karger; 2009.
23. Savage JR. Classification and relationships of induced chromosomal structual changes. *J Med Genet.* 1976;13(2):103-122.
24. Salmena L, Hakem R. Caspase-8 deficiency in T cells leads to a lethal lymphoinfiltrative immune disorder. *J Exp Med.* 2005;202(6):727-732.
25. Kovalchuk AL, Kim JS, Park SS, et al. IL-6 transgenic mouse model for extraosseous plasmacytoma. *Proc Natl Acad Sci U S A.* 2002;99(3):1509-1514.
26. Nishimoto N, Kishimoto T. Interleukin 6: from bench to bedside. *Nat Clin Pract Rheumatol.* 2006;2(11):619-626.
27. Hong DS, Angelo LS, Kurzrock R. Interleukin-6

and its receptor in cancer: implications for Translational Therapeutics. *Cancer.* 2007;110(9):1911-1928.

28. Bouillet P, Metcalf D, Huang DC, et al. Proapoptotic Bcl-2 relative Bim required for certain apoptotic responses, leukocyte homeostasis, and to preclude autoimmunity. *Science.* 1999; 286(5445):1735-1738.
29. Tomita S, Sinal CJ, Yim SH, Gonzalez FJ. Conditional disruption of the aryl hydrocarbon receptor nuclear translocator (Arnt) gene leads to loss of target gene induction by the aryl hydrocarbon receptor and hypoxia-inducible factor 1alpha. *Mol Endocrinol.* 2000;14(10):1674-1681.
30. Chan IT, Kutok JL, Williams IR, et al. Conditional expression of oncogenic K-ras from its endogenous promoter induces a myeloproliferative disease. *J Clin Invest.* 2004;113(4):528-538.
31. Heilman SA, Kuo YH, Goudswaard CS, Valk PJ, Castilla LH. Cbfbeta reduces Cbfbeta-SMMHC-associated acute myeloid leukemia in mice. *Cancer Res.* 2006;66(23):11214-11218.
32. Greenblatt MS, Bennett WP, Hollstein M, Harris CC. Mutations in the p53 tumor suppressor gene: clues to cancer etiology and molecular pathogenesis. *Cancer Res.* 1994;54(18):4855-4878.
33. Junttila MR, Evan GI. p53–a Jack of all trades but master of none. *Nat Rev Cancer.* 2009;9(11):821-829.
34. Holland AJ, Cleveland DW. Boveri revisited: chromosomal instability, aneuploidy and tumorigenesis. *Nat Rev Mol Cell Biol.* 2009;10(7):478-487.
35. Fukasawa K. Oncogenes and tumour suppressors take on centrosomes. *Nat Rev Cancer.* 2007;7(12):911-924.
36. Sagona AP, Stenmark H. Cytokinesis and cancer. *FEBS Lett.* 2010;584(12):2652-2661.
37. Steigemann P, Wurzenberger C, Schmitz MH, et al. Aurora B-mediated abscission checkpoint protects against tetraploidization. *Cell.* 2009; 136(3):473-484.
38. Krelin Y, Zhang L, Kang TB, Appel E, Kovalenko A, Wallach D. Caspase-8 deficiency facilitates cellular transformation in vitro. *Cell Death Differ.* 2008; 15(9):1350-1355.
39. Fenech M, Kirsch-Volders M, Natarajan AT, et al. Molecular mechanisms of micronucleus, nucleoplasmic bridge and nuclear bud formation in mammalian and human cells. *Mutagenesis.* 2011; 26(1):125-132.
40. Lengauer C, Kinzler KW, Vogelstein B. Genetic instabilities in human cancers. *Nature.* 1998; 396(6712):643-649.
41. Ganem NJ, Godinho SA, Pellman D. A mechanism linking extra centrosomes to chromosomal instability. *Nature.* 2009;460(7252):278-282.
42. Riley T, Sontag E, Chen P, Levine A. Transcriptional control of human p53-regulated genes. *Nat Rev Mol Cell Biol.* 2008;9(5):402-412.
43. Kaiser WJ, Upton JW, Long AB, et al. RIP3 mediates the embryonic lethality of caspase-8-deficient mice. *Nature.* 2011;471(7338):368-372.
44. Oberst A, Dillon CP, Weinlich R, et al. Catalytic activity of the caspase-8-FLIP(L) complex inhibits RIPK3-dependent necrosis. *Nature.* 2011; 471(7338):363-367.
45. Ch'en IL, Beisner DR, Degterev A, et al. Antigen-mediated T cell expansion regulated by parallel pathways of death. *Proc Natl Acad Sci U S A.* 2008;105(45):17463-17468.
46. Schvartzman JM, Sotillo R, Benezra R. Mitotic chromosomal instability and cancer: mouse modelling of the human disease. *Nat Rev Cancer.* 2010;10(2):102-115.